



Published in final edited form as:

Stem Cells. 2016 June ; 34(6): 1513–1526. doi:10.1002/stem.2332.

Molecular analysis of neutrophil differentiation from human iPSCs delineates the kinetics of key regulators of hematopoiesis

Colin L. Sweeney^{1,*}, Ruifeng Teng^{2,*}, Hongmei Wang^{1,*}, Randall K. Merling¹, Janet Lee¹, Uimook Choi¹, Sherry Koontz¹, Daniel G. Wright², and Harry L. Malech¹

¹Laboratory of Host Defenses, National Institute of Allergy and Infectious Diseases, National Institutes of Health, Bethesda, MD 20817 USA

²The Molecular Medicine Branch, National Institute of Diabetes and Digestive and Kidney Diseases, National Institutes of Health, Bethesda, MD 20817 USA

Abstract

In vitro generation of mature neutrophils from human induced pluripotent stem cells (iPSCs) requires hematopoietic progenitor development followed by myeloid differentiation. The purpose of our studies was to extensively characterize this process, focusing on the critical window of development between hemogenic endothelium, hematopoietic stem/progenitor cells (HSPCs), and myeloid commitment, to identify associated regulators and markers that might enable the stem cell field to improve the efficiency and efficacy of iPSC hematopoiesis. We utilized a 4-stage differentiation protocol involving: embryoid body (EB) formation (Stage-1); EB culture with hematopoietic cytokines (Stage-2); HSPC expansion (Stage-3); and neutrophil maturation (Stage-4). CD34⁺CD45⁻ putative hemogenic endothelial cells were observed in Stage-3 cultures, and expressed VEGFR-2/Flk-1/KDR and VE-cadherin endothelial markers, GATA-2, AML1/RUNX1, and SCL/TAL1 transcription factors, and endothelial/HSPC-associated microRNAs miR-24, miR-125a-3p, miR-126/126*, and miR-155. Upon further culture, CD34⁺CD45⁻ cells generated CD34⁺CD45⁺ HSPCs that produced hematopoietic CFUs. Mid-Stage-3 CD34⁺CD45⁺ HSPCs exhibited increased expression of GATA-2, AML1/RUNX1, SCL/TAL1, C/EBP α , and PU.1 transcription factors, but exhibited decreased expression of HSPC-associated microRNAs, and failed to engraft in immune-deficient mice. Mid-stage-3 CD34⁺CD45⁺ cells maintained PU.1 expression and exhibited increased expression of hematopoiesis-associated miR-142-3p/5p and a trend towards increased miR-223 expression, indicating myeloid commitment. By late Stage-4, increased CD15, CD16b, and C/EBP ϵ expression were observed, with 25–65% of cells exhibiting morphology and functions of mature neutrophils. These studies demonstrate that hematopoiesis and neutrophil differentiation from human iPSCs recapitulates many features of embryonic

Corresponding author: Harry L. Malech, MD; LHD/NIAID/NIH; Bldg 10, Rm 5-3750, 10 Center Dr, MSC-1456; Bethesda, MD 20892-1456, ; Email: hmalech@nih.gov; Tel: 240-447-4924; Fax: 301-402-0789

*These authors contributed equally to this work

Disclosure of Potential Conflicts of Interest: The authors indicate no potential conflicts of interest.

Author Contributions:

CLS: Collection, assembly, analysis, and interpretation of data; manuscript writing. RT: Conception and design; collection, assembly, and analysis of data. HW: Conception and design; collection, assembly, and analysis of data; manuscript writing. RKM, JL, UC, SK: Collection and assembly of data. DGW: Assembly, analysis, and interpretation of data, financial support. HLM: Conception and design, data analysis and interpretation, financial support.

hematopoiesis and neutrophil production in marrow, but reveals unexpected molecular signatures that may serve as a guide for enhancing iPSC hematopoiesis.

Keywords

human induced pluripotent stem cells; microRNA; transcription factors; CD34 antigen; hematopoietic stem cells; neutrophils

Introduction

The use of induced pluripotent stem cells (iPSCs) in research and as potential therapies requires a full understanding of the ontogeny of *in vitro* development of these cells into differentiated cells and tissues. Our laboratory has a longstanding interest in developing genetic and pharmacologic treatments for inherited disorders affecting the function or production of neutrophils, which can be modeled *in vitro* using patient derived iPSCs.

Human embryonic stem cells (ESCs) or iPSCs can be differentiated *in vitro* to mature cells of multiple hematopoietic lineages, including erythrocytes, macrophages, B-cells, T-cells, megakaryocytes, and neutrophils [1–11], through processes recapitulating many aspects of embryonic hematopoietic development. In both mice and humans, primitive hematopoiesis is initiated in the extraembryonic yolk sac [12, 13]. After the first wave of primitive hematopoiesis, definitive hematopoietic stem/progenitor cells (HSPCs) can be detected in the embryonic aorta-gonado-mesonephros (AGM) region. Both yolk sac and AGM hematopoiesis originate from cells demonstrating hematopoietic and endothelial potential, termed hemangioblasts or hemogenic endothelium [14–16]. In human ESC differentiation studies, such cells have been found in the CD34⁺CD45[−] population [13] expressing Flk-1 (VEGFR-2) [17] and CD31 [18]. Upon further differentiation, CD45 is expressed in hematopoietic lineages. Among both somatic cells and cells derived from human pluripotent stem cells, CD34⁺CD45⁺ cells are enriched for clonogenic HSPCs possessing the capacity to generate multiple mature hematopoietic lineages, as in methylcellulose CFU assays.

Despite success in generating mature hematopoietic lineages from human pluripotent stem cells, there has been less progress towards developing techniques for *in vitro* generation of HSPCs that are capable of robust long-term multilineage repopulation *in vivo*, with few studies demonstrating even limited hematopoietic engraftment and reconstitution in immune-deficient mouse transplants [19–22]. It has been reported that teratomas formed by human iPSCs subcutaneously injected in immune-deficient mice can generate small numbers of human HSPCs that are capable of engraftment upon subsequent transplant into additional immune-deficient mice [23]. Moreover, teratomas formed by co-injection of OP9 cells with human iPSCs exhibited enhanced development of both myeloid cells and transplantable HSPCs, particularly with OP9 cells expressing Wnt3a transgene. Wnt3a has also been shown to enhance development of functional neutrophils from iPSCs of patients with severe congenital neutropenia [24]. More recently, *in vitro* co-culture of primate iPSC-derived CD34⁺ cells with human umbilical cord endothelial cells expressing Notch ligands was shown to enhance long term hematopoietic engraftment in immunodeficient mice [25]. These studies demonstrated that human iPSCs are not intrinsically defective for production

of engraftable HSPCs, depending on the conditions used for hematopoietic differentiation, and that maneuvers such as exposure to Wnt3a or Notch ligand could improve the efficiency of HSPC differentiation and myelopoiesis from iPSCs.

In order to identify additional molecular factors that are associated with the regulation or identity of human iPSC-derived hematopoietic cell lineages, we utilized a 32-day 4-stage discontinuous culture system that we previously described as supporting the generation of functionally mature neutrophils from human iPSCs *in vitro* [10], which was adapted from Yokoyama's ESC system [9], and which we previously utilized to demonstrate safe harbor targeted minigene correction of iPSCs from patients with chronic granulomatous disease by restoring oxidase activity in differentiated neutrophils [11]. This culture system allows for the generation of a high percentage of mature neutrophils (25–65%) following the emergence of HSPCs.

The present study delineates the kinetics of hematopoietic clonogenicity and expression of surface markers, transcription factors, and 754 microRNAs during HSPC and neutrophil differentiation in this iPSC culture system, and identifies relationships between lineage commitment, phenotype, and the expression of microRNAs and transcription factors that recapitulate features of the embryonic development of hematopoietic tissues and production of neutrophils in marrow. These analyses may provide the stem cell research community with a roadmap for developing tools to improve the efficiency and efficacy of hemogenic endothelial and hematopoietic differentiation from iPSCs.

Material and Methods

Human subjects

All human subjects providing peripheral blood signed written informed consent allowing these studies following the Declaration of Helsinki under the National Institute of Allergy and Infectious Diseases Institutional Review Board approved NIH protocol 05-I-0213.

iPSC source and maintenance

Human iPSCs in this study included peripheral blood CD34⁺ HSPC-derived iNC-01-3, iNC-01-4, and iNC-01-12 [26], and fibroblast-derived iPS(IMR90)-1 [27] (WiCell, Madison, WI, USA). iPSCs were cultured at 37°C, 5% CO₂, on mitomycin C-treated mouse embryonic fibroblasts as previously described [26].

Differentiation of mature neutrophils from human iPSCs by 4-stage discontinuous culture

4-stage discontinuous culture for generation of neutrophils from iPSCs (Fig. 1A) was performed as previously described [9–11].

Stage-1 embryoid body (EB) formation was initiated on day 0 from iPSCs seeded to ultra-low attachment dishes (Corning, Tewksbury, MA, USA) in StemSpan SFEM (STEMCELL Technologies, Vancouver, BC, Canada) with 10 μM Y-27632 ROCK inhibitor (Merck Millipore, Billerica, MA) overnight. Results labeled day 0 refer to analyses of undifferentiated iPSCs.

Stage-2 was initiated on day 1 by changing medium to IMDM (Life Technologies, Grand Island, NY, USA) containing 15% HyClone fetal bovine serum (FBS; Thermo Scientific, Waltham, MA, USA), 1% NEAA, 2mM L-glutamine, 100U/mL penicillin/streptomycin (Life Technologies), and 0.1mM β -mercaptoethanol plus human cytokines: bone morphogenetic protein-4 (25ng/mL; R&D Systems, Minneapolis, MN), stem cell factor (SCF, 50ng/mL), Flt-3 ligand (50ng/mL), interleukin-6 (IL-6, 50ng/mL) and thrombopoietin (TPO, 20ng/mL; PeproTech, Rocky Hill, NJ, USA). EBs were cultured in this hematopoietic induction media for 17 days (labeled days 2 to 18).

For Stage-3, EBs were dissociated on day 18 with 0.25% Trypsin/EDTA and plated onto irradiated (15Gy) murine OP9 marrow stromal cells (ATCC, Manassas, VA, USA) in IMDM supplemented with 10% FBS, 10% horse serum (STEMCELL Technologies), 5% protein-free hybridoma medium (Life Technologies), 100U/mL penicillin/streptomycin, 0.1mM β -mercaptoethanol, 100ng/mL SCF, 100ng/mL Flt-3 ligand, 100ng/mL IL-6, 10ng/mL TPO and 10ng/mL human interleukin-3 (PeproTech). Results labeled days 19 to 25 refer to analyses of non-adherent cells (harvested by gentle pipeting), unless otherwise indicated that the adherent cell layer (harvested using trypsin/EDTA) was analyzed after removal of non-adherent cells.

For Stage-4, non-adherent cells were transferred on day 25 onto new irradiated OP9 cells for 7 days culture in IMDM with 10% FBS, 100U/mL penicillin, 100 μ g/mL streptomycin, 0.1mM β -mercaptoethanol, and 50ng/mL human granulocyte colony-stimulating factor (G-CSF; Neupogen; Amgen, Thousand Oaks, CA). Results labeled days 26 to 32 refer to analyses of non-adherent cells.

Neutrophil morphology and function

Cells from the end of Stage-4 culture were cytospun at 70x g for 5 minutes using a Cytospin 3 (Thermo Scientific), fixed with methanol for 5–7 minutes, stained for 15 to 30 minutes with modified Giemsa stain (Sigma-Aldrich, St. Louis, MO), and rinsed with deionized water. Dihydrorhodamine-123 (DHR) analysis of oxidase activity and zymosan analysis of neutrophil phagocytic capacity were performed as previously described [10, 11].

Cell surface marker analyses

Cells were labeled with fluorescein isothiocyanate (FITC)-conjugated anti-human (h)CD15 or hCD45 antibodies; phycoerythrin-cyanin5 (PE-Cy5)-conjugated anti-hCD45 or hCD33; allophycocyanin (APC)-conjugated hCD34; and/or phycoerythrin (PE)-anti-hCD34, hVEGFR-2/Flk-1/KDR, hVE-cadherin, or hCD16b (BD Biosciences, San Jose, CA). Surface marker expression was analyzed and cell subpopulations were sorted with a FACSCanto or FACSCalibur flow cytometer (BD Biosciences).

Transcription factor analysis

Total RNA was extracted with RNeasy Total Purification Kit (Bio-Synthesis, Lewisville, TX) and cDNA was produced using SuperScript First-Strand Synthesis System (Life Technologies). Real-time PCR was performed with TaqMan Universal PCR Master Mix on an ABI 7500 system (Applied Biosystems; Life Technologies). Gene-specific primers and

probes were from Applied Biosystems: GATA-2 (Hs 00231119_m1), SCL/TAL1 (Hs 00268434_m1), AML1/RUNX1 (Hs00231079_m1), C/EBP α (Hs 00269972_s1), C/EBP ϵ (Hs 00357657_m1) and PU.1 (Hs 00231368_m1). Transcription factor cDNAs and beta-2-microglobulin controls for each sample were amplified in duplicate. Comparative quantification of each transcription factor was performed based on cycle threshold (CT) normalized to beta-2-microglobulin relative to expression in undifferentiated iPSCs using CT.

Methylcellulose colony forming unit (CFU) assay

For initial CFU assays, single cell suspensions of whole non-adherent populations from Stage-3 were plated in triplicate at 100,000 cells in 1.5ml of MethoCult H4535 (without EPO; STEMCELL Technologies) per 35mm dish. Cells were incubated for 14 days in a humidified incubator at 37°C with 5% CO₂ and evaluated for colonies by bright field microscopy. For CFU assays of sorted Stage-3 cell populations, CD34⁺CD45⁺ cells were used directly (day 22) or CD34⁺CD45⁻ cells were cultured for 7 additional days in Stage-3 medium then sorted for CD34⁺CD45⁺ (day 22+7). For each population, 500 or 1000 CD34⁺CD45⁺ cells were plated per 35mm dish in MethoCult H4434 (with EPO; STEMCELL Technologies) and cultured for 14 days as above.

Statistical analyses

For surface marker, transcription factor, and CFU analyses, one-way ANOVA or unpaired two-tailed t-test were performed using GraphPad Prism version 6.0 for Mac (GraphPad Software, La Jolla, CA).

MicroRNA expression assay

Undifferentiated iPSCs (n=5), day 18 EBs (n=2), and Stage-3 day 22 sorted CD34⁺CD45⁻ adherent cells, CD34⁺CD45⁺ cells, and CD34⁻CD45⁺ cells (n=3 each) were prepared from iNC-01-3 and iNC-01-4 iPSCs. Samples were disrupted in denaturing lysis buffer and total RNA was purified using *mirVana* miRNA Isolation Kit (Applied Biosystems). MicroRNA cDNA was synthesized from total RNA using TaqMan MicroRNA Reverse Transcription Kit with Megaplex RT primers (pool A and B), followed by two unbiased preamplification reactions (Megaplex PreAmp primers pool A and B; Applied Biosystems). Expression analysis of 754 microRNAs was performed with TaqMan Human MicroRNA Array A+B v3.0 on an ABI 7900HT system using ExpressionSuite software v1.0.3 (Applied Biosystems) for comparative CT analysis normalized to U6 snRNA and RNU48 control RNAs relative to expression in undifferentiated iPSCs; for each microRNA, replicates with an undetermined CT were omitted by the software analysis, based on a presumed technical failure of that assay. Statistical analysis was performed using ExpressionSuite software two-tailed Student's t-test. MicroRNA expression data was deposited in Gene Expression Omnibus with accession number GSE69503 (<http://www.ncbi.nlm.nih.gov/geo/query/acc.cgi?acc=GSE69503>).

Results

Differentiation and characterization of functional mature neutrophils from human iPSCs

4-stage differentiation of iPSCs to neutrophils was performed as described in Materials and Methods and Figure 1A. At the end of Stage-4, 25–65% of non-adherent cells exhibited mature neutrophil morphology (Fig. 1B), with macrophages, eosinophils, and myeloid precursors also present. The end-stage cell population demonstrated neutrophil-associated oxidative burst activity by DHR assay (Fig. 1C) and the ability to phagocytize opsonized zymosan (Fig. 1D), in addition to the antimicrobial and *in vivo* homing functions of mature neutrophils that we previously reported using this differentiation protocol [10].

Kinetics of cell surface antigen expression

To further characterize the process of neutrophil differentiation from iPSCs, we analyzed surface marker expression on cells arising during 4-stage iPSC differentiation cultures (Fig. 2). Except for very low expression of CD15/Lewis X/SSEA-1 antigen in a small subset of undifferentiated iPSCs, no hematopoietic surface markers were detected in undifferentiated iPSCs. CD34 antigen, which is expressed on hemangioblasts, some endothelial cells, and HSPCs that give rise to mature cells of multiple hematopoietic lineages, could be detected in small numbers of differentiating cells by day 3, peaking at 11% CD34⁺ by day 10 (midway through Stage-2) and then declining through the end of Stage-2 (Fig. 2A, 2B). CD34⁺ cells appearing during early to mid-Stage-2 cultures lacked expression of the CD45 pan-leukocyte marker, consistent with early hemangioblasts or hemogenic endothelium. Following the emergence of rare CD34⁺CD45⁺ cells in late Stage-2, expression of CD33 myeloid-specific marker and CD45 also was detected, with 6–10% of cells becoming weakly positive by day 18.

Following transition of cultures to Stage-3 on day 18, the majority of EB-derived cells adhered tightly to the OP9 feeder layer. On day 18 prior to OP9 co-culture, most CD34⁺ cells also expressed endothelial progenitor markers VE-cadherin and VEGFR-2/Flk-1/KDR (Fig. 3A and 3B; left-most panels), and were CD45[−] (not shown). By 4 hours after transfer of dissociated EBs onto OP9 feeder cells, a distinction was evident between endothelial marker expression in the majority of adherent CD34⁺ cells (Fig. 3A and 3B; lower graph series in each) versus no expression in the majority of non-adherent CD34⁺ cells (Fig. 3A and 3B; upper graph series in each). This became more accentuated over the next 4 days of Stage-3.

During early Stage-3, the percentage of CD34⁺ non-adherent cells rapidly increased, peaking at 30–40% of non-adherent cells at day 20 (Fig. 2B), and then decreased significantly thereafter ($p < 0.0001$ by ANOVA). Throughout Stage-3 and Stage-4, nearly 100% of non-adherent CD34⁺ cells also co-expressed CD45 (Fig. 2A, 2B), marking them as putative HSPCs. The percentage of CD45⁺ and CD33⁺ non-adherent cells also rapidly increased during Stage-3 (Fig. 2A, 2B) to almost 100% by day 22, remaining so through the end of Stage-4, suggesting rapid progression towards myeloid differentiation from HSPCs. Expression of the late differentiation myeloid antigen CD15 and neutrophil-specific antigen CD16b increased progressively in non-adherent cells during Stage-3, plateauing by the end

of Stage-4 (Fig. 2A, 2B) when cells exhibiting mature neutrophil morphology and functions were observed (Fig. 1).

Expression kinetics of transcription factors

We performed quantitative reverse-transcription PCR analysis of transcription factors involved in hematopoietic commitment throughout the 4-stage culture (Fig. 4A). Baseline expression of GATA-2, AML1/RUNX1 and C/EBP α was detected in iPSCs, and increased by approximately 4 to 8-fold to peak levels early during Stage-2 at around day 3. Similarly, SCL/TAL1 also increased in Stage-2, but peaked later at around day 10 (Fig. 4A), when the initial peak of CD34⁺CD45⁻ cells was also observed (Fig. 2B). GATA-2, AML1/RUNX1, C/EBP α and SCL/TAL1 expression decreased slowly from peak levels during subsequent culture stages, but with a modest spike of SCL/TAL1 and AML1/RUNX1 expression at day 20 (Fig. 4A), concomitant with a peak of CD34⁺CD45⁺ cells (Fig. 2B). GATA-2 and SCL/TAL1 were undetectable by late Stage-4.

PU.1 is a master transcription factor regulating development of both granulocytes and monocytes/macrophages [28–30]. During iPSC differentiation, PU.1 expression began to increase at mid-Stage-2, peaking at day 20 in non-adherent cells early after transition to Stage-3 culture (Fig. 4A). There was a second smaller peak in PU.1 expression at day 27 after transition to Stage-4 culture with the addition of G-CSF, with maintenance of PU.1 expression thereafter. Expression of the late-myeloid transcription factor C/EBP ϵ began to increase at day 20 and peaked following transition to Stage-4 culture, with the highest levels of expression observed on day 28 (Fig. 4A) when 90–95% of cells expressed CD15 and CD16b (Fig. 2B).

Due to asynchronous differentiation, cells of varying hematopoietic stages and lineages were present together in cultures at the same time-points and on multiple days during Stage-3 and Stage-4. To compare transcription factor expression between different subpopulations and days, we used surface co-expression of either CD34/CD45 or CD15/CD33 to FACS-sort and analyze putative hemogenic endothelium (CD34⁺CD45⁻), putative HSPCs (CD34⁺CD45⁺), and their maturing hematopoietic progeny (CD34⁻CD45⁺) at days 18 and 22, and myeloid lineage cells (CD15⁺CD33⁺) at day 22 and 28. Transcription factors GATA-2, AML1/RUNX1 and SCL/TAL1 were significantly increased in expression in day 22 CD34⁺CD45⁻ putative hemogenic endothelium compared to day 0 iPSCs (GATA-2 and AML/RUNX1: $p < 0.01$; SCL/TAL1: $p < 0.0001$ by t-test), and were further increased in day 22 CD34⁺CD45⁺ presumptive HSPCs (GATA-2 and AML/RUNX1: $p < 0.0005$; SCL/TAL1: $p < 0.005$ by t-test, compared to day 22 CD34⁺CD45⁻), but were significantly decreased in CD34⁻CD45⁺ cells on day 22 ($p = 0.001$ by t-test) and CD15⁺CD33⁺ cells on days 22 and 28 ($p = 0.0005$ by t-test) compared to day 22 CD34⁺CD45⁺ (Fig. 4B). Early myeloid transcription factors C/EBP α and PU.1 were significantly increased in the day 22 CD34⁺CD45⁺ population compared to day 22 CD34⁺CD45⁻ cells (C/EBP α : $p = 0.0005$; PU.1: $p < 0.0001$ by t-test). PU.1 expression was maintained in CD34⁻CD45⁺ cells and CD15⁺CD33⁺ cells, while C/EBP α decreased significantly in late Stage-4 day 28 CD15⁺CD33⁺ cells compared to day 22 CD34⁺CD45⁺ cells ($p < 0.005$ by t-test). C/EBP ϵ expression over background iPSC levels was only detected

in CD15⁺CD33⁺ cells (Fig. 4B), consistent with previous reports that C/EBP ϵ is exclusively expressed in granulocytes [31, 32].

Kinetics of hematopoietic colony forming potential

In order to characterize the clonogenic potential of hematopoietic cells arising during 4-stage cultures, we performed methylcellulose colony assays on unsorted cells to determine when HSPCs with CFU activity emerged. In parallel, cells were analyzed by flow cytometry for an HSPC phenotype (CD34⁺CD45⁺). Consistent with the results described above (Fig. 2A and 2B), only ~1% of cells were CD34⁺CD45⁺ at the end of Stage-2 on day 18 (Fig. 5A), but CD34⁺CD45⁺ cells constituted ~30% of non-adherent cells in Stage-3 cultures at day 20, significantly decreasing in numbers thereafter ($p < 0.0001$ by ANOVA), and becoming undetectable by day 28. Concomitantly, CFU activity, nearly undetectable at day 18 (Fig. 5B), peaked at days 20 and 22 at approximately 450 CFU/100,000 unsorted cells, decreasing significantly thereafter ($p < 0.0001$ by ANOVA), and becoming undetectable by day 28. This indicated that the emergence of hematopoietic CFUs during iPSC differentiation coincided with the appearance of CD34/CD45 antigen co-expression, although peak CFU activity persisted in day 22 populations in which CD34⁺CD45⁺ cells decline.

For further characterization of the hematopoietic potential of Stage-3 cells, CD34⁺CD45⁺ non-adherent cells and CD34⁺CD45⁻ adherent cells were sorted from Stage-3 day 22 cultures (Fig. 5C and 5D). When sorted CD34⁺CD45⁻ adherent cells were cultured for an additional 7 days in Stage-3 medium without OP9 cells (day 22+7 culture), >80% of cells became CD45⁺ (Fig. 5E), indicating that the CD34⁺CD45⁻ adherent population included hemogenic cells capable of giving rise to putative HSPCs. Sorted CD34⁺CD45⁺ cells from both day 22 and day 22+7 cultures were capable of forming hematopoietic CFUs in methylcellulose assays (Fig. 5F), with a CFU frequency of 1/115 to 1/47 for the day 22 sorted cells compared to a CFU frequency of 1/20 for the day 22+7 sorted cells, confirming HSPC activity of these CD34⁺CD45⁺ populations. CFUs detected in these assays were predominantly CFU-GM (Fig. 5G), and CFU-E or BFU-E were not observed.

Despite *in vitro* CFU potential, intra-femoral injection of CD34⁺CD45⁺ cells into immunodeficient NSG mice resulted in no detectable human CD45⁺ hematopoietic cells at 8 weeks post-transplant (Supplemental Figure S1). This result is consistent with the failure to generate long-term engrafting HSPCs from human pluripotent stem cells that has been reported with numerous *in vitro* differentiation protocols based on EBs and/or co-culture with marrow stromal cells [1, 18, 19, 33].

MicroRNA expression in cell populations with hematopoietic potential

To assess microRNA expression in differentiated cells present at time-points when HSPCs with CFUs activity were detectable, we analyzed Stage-2 day 18 EBs and sorted populations of cells from mid-Stage-3 (day 22) cultures: adherent CD34⁺CD45⁻ cells (containing hemogenic endothelium), non-adherent CD34⁺CD45⁺ HSPCs, and non-adherent CD34⁻CD45⁺ cells. Expression of 754 microRNAs in these populations was compared to undifferentiated iPSCs. MicroRNAs for which expression was significantly increased or

decreased ($p < 0.05$) in one or more of the day 22 sorted populations compared to iPSCs are shown in Table 1 and Supplemental Figure S2.

As expected, decreased expression of pluripotency-associated microRNAs was observed in day 18 EBs and in sorted cells from day 22 cultures (Table 1 and Supplemental Figure S2), including the miR-302/367 cluster family members miR-302a*, miR-302b, miR-302c, miR-302d, and miR-367 [34, 35], and miR-372 [36]. MicroRNAs with significantly increased expression in adherent CD34⁺CD45⁻ cells relative to iPSCs included endothelial- and HSPC-associated miR-24, miR-125a-3p, miR-126/126*, and miR-155, as well as erythropoiesis-associated miR-144. Non-adherent CD34⁺CD45⁺ cells also exhibited significantly increased expression of miR-144 but did not have significantly increased expression of HSPC-associated microRNAs relative to iPSCs. Non-adherent CD34⁻CD45⁺ cells expressed significantly increased levels of HSPC-associated let-7e and hematopoiesis-associated miR-142-3p and miR-142-5p compared to undifferentiated iPSCs, and significantly decreased expression of miR-130a, which has been reported to decrease during neutrophil differentiation from myeloblasts and promyelocytes [37], consistent with the beginning of myeloid and neutrophil commitment in this cell population.

Day 22 sorted cells also exhibited significantly altered expression of additional microRNAs not previously associated with hematopoiesis or pluripotency (Table 1 and Supplemental Figure S2). These include a subset of microRNAs with distinct population-specific patterns of increased expression: miR-139-5p, miR-497, miR-938, and miR-1289 which exhibited peak expression in CD34⁺CD45⁻ cells, and miR-938 which exhibited peak expression in CD34⁺CD45⁺ cells (Supplemental Figure S3). Of these, the tumor-suppressors miR-139-5p [38–40] and miR-497 [41–44] have been reported to inhibit metastasis or regulate cell cycle progression, respectively, in a variety of cell types. MiR-628-3p expression has been reported as increased or decreased in a variety of cancers [45–48], but its function has not been defined. MiR-938 expression has been associated with inhibition of *Smad3* expression in TGF- β signaling in pituitary adenomas [49]. MiR-1289 has been associated with the localization of target mRNAs into microvesicles [50]. These functions, or others not yet described for this subset of microRNAs, may delineate important properties of the hematopoietic-associated cell populations characterized in the present study.

Expression patterns of a subset of hematopoiesis-associated microRNAs in iPSCs, day 18 EBs, and day 22 sorted cell populations are shown in Figure 6. CD34⁺CD45⁺ cells exhibited lower mean levels of HSPC-associated let-7e, miR-24, miR-125a-3p, miR-126/126*, and miR-155 compared to adherent CD34⁺CD45⁻ cells and levels of hematopoietic-associated miR-142-3p/5p intermediate between CD34⁺CD45⁻ and CD34⁻CD45⁺ cells. MiR-142-3p and miR-142-5p expression are specific to all hematopoietic cells [51], and increase as HSPCs differentiate towards myeloid cells and other hematopoietic lineages [52–54], consistent with the higher expression levels in CD34⁻CD45⁺ cells compared to CD34⁺CD45⁺ HSPCs. Increased expression of myeloid-associated miR-223 [55, 56] was also observed in CD34⁺CD45⁺ and CD34⁻CD45⁺ cells, but fell short of the statistical significance threshold ($p < 0.05$) applied to the microRNA expression analysis. Together, these microRNA expression profiles suggest a decrease in HSPC potential and the beginning

of myeloid commitment in day 22 CD34⁺CD45⁺ cells prior to maturation into CD34⁺CD45⁺ cells and subsequent granulocyte differentiation.

Discussion

Differentiation of human iPSCs through early HSPC development to mature myeloid cells offers a novel opportunity to study both hematopoiesis and the modeling of neutrophil disorders *in vitro* [11, 24]. In the current study, we utilized a 32-day 4-stage *in vitro* culture protocol that supports the generation of mature neutrophils from iPSCs to analyze the kinetics of hematopoietic surface marker and transcription factor expression associated with normal hematopoietic and myeloid cell development. Through analyses of intermediary cell stages that emerged in 4-stage cultures, we characterized the early development of primitive hemangioblasts or hemogenic endothelium from iPSCs and the subsequent appearance of cells with HSPC surface markers (CD34⁺CD45⁺) and clonogenic potential. We also evaluated the expression of 754 microRNAs in embryoid bodies, endothelial cells with hemogenic potential, and hematopoietic cell populations arising in this culture system, to further characterize molecular signatures of iPSC-derived cells at different stages of hematopoietic and myeloid development.

In our study, progression of iPSC differentiation towards neutrophils was evident by changes in surface marker expression, cell morphology, and function, recapitulating many aspects of early embryonic hematopoietic development and marrow granulopoiesis. During early Stage-2, small numbers of cells initially emerged expressing CD34 without CD45, and expressed VEGFR-2 and VE-cadherin endothelial markers by late Stage-2, likely representing hemangioblasts or hemogenic endothelium as in human ESC studies. Transition to Stage-3 co-culture with OP9 cells greatly enhanced generation of non-adherent CD34⁺CD45⁺ HSPCs that likely emerged from CD34⁺CD45⁺ adherent hemogenic endothelium, since purified day 22 CD34⁺CD45⁺ adherent cells were shown to generate non-adherent CD34⁺CD45⁺ cells when sorted into new cultures. The kinetics of generation of CD34⁺CD45⁺ HSPCs closely paralleled the kinetics of development of clonogenic hematopoietic progenitors based on CFU assays. However, HSPCs and clonogenic hematopoietic progenitors did not persist in culture, but instead progressively differentiated into more mature hematopoietic cells, with an abrupt disappearance of CD34 and emergence of myeloid (CD33) and neutrophil markers (CD15 and CD16b).

Hematopoietic differentiation requires temporal regulation of transcription factors and signaling pathways that, if manipulated, may help instruct an HSPC fate from iPSCs. These include Wnt [57], Notch [58], and bone morphogenetic protein signaling [59], as well as expression of GATA-2, SCL/TAL1, and AML1/RUNX1 transcription factors [60–63]. GATA-2 is thought to be important in early hematopoiesis but is not required for terminal differentiation [60]. We observed that GATA-2 increased early in differentiation, and decreased prior to the appearance of CD15 neutrophil marker. SCL/TAL1 appears to be the most reliable transcription factor for tracking early hematopoietic commitment and is expressed in all hemogenic embryonic tissues [62, 63]. SCL/TAL1 regulates erythroid and megakaryocytic differentiation, and SCL/TAL1^{-/-} mice exhibit embryonic lethality with lack of blood formation [64]. In the current study, SCL/TAL1 expression increased during

early Stage-2, peaking at day 10, indicating conversion of mesoderm to hemogenic progenitors. The second wave of SCL/TAL1 appeared at day 20 when CD34⁺CD45⁺ cell percentages peaked. AML1/RUNX1 was also expressed in waves, the first peaking at day 3 and the second at day 20 of differentiation. At day 18 and 20, AML1/RUNX1 expression was highest in CD34⁺CD45⁺ cells, but was also expressed at lower levels in CD34⁺CD45⁻ cells containing hemogenic endothelium, consistent with previous reports that SCL and AML1/RUNX1 are expressed in hemangioblasts during EB differentiation from mouse ESCs [65, 66].

C/EBP α and PU.1 are critical for hematopoietic commitment to a neutrophil/monocyte progenitor and progression to mature neutrophils and monocytes [67]. C/EBP ϵ plays an important role in late neutrophil maturation; C/EBP ϵ -deficient mice lack secondary and tertiary granules (indicating defective progression from myeloblasts to promyelocytes and myelocytes) and C/EBP ϵ mutations are associated with neutrophil-specific granule deficiency in humans [32]. In our iPSC differentiation culture, C/EBP ϵ expression appeared later than C/EBP α and was detected only in CD15⁺ cells, while PU.1 expression was up-regulated in CD34⁺CD45⁺ cells and was retained during subsequent myeloid maturation.

MicroRNAs are a class of small noncoding RNAs that can silence expression of target genes post-transcriptionally by regulating mRNA translation or stability [68], and play important roles in governing lineage commitment of hematopoietic progenitors [69]. In our analysis of sorted cell populations in Stage-3 differentiation cultures relative to undifferentiated iPSCs, the majority of the microRNAs detected at significantly increased levels in these cell populations had not previously been associated with hematopoietic identity. These microRNAs may provide additional insight into the differences between iPSC-derived hematopoietic populations and their somatic counterparts. Further functional studies are warranted to assess their roles in hematopoietic differentiation and determine whether their manipulation can influence hematopoietic differentiation from human iPSCs.

MicroRNAs expressed at significantly increased levels in day 22 CD34⁺CD45⁻ adherent cells relative to undifferentiated iPSCs included miR-24, miR-125a-3p, miR-126/126*, and miR-155. Expression of miR-125a [70–72], miR-126/126* [73–75], and miR-155 [76, 77] are associated with both endothelial cells and HSPCs. MiR-125a is expressed in a tricistronic transcript with miR-99b and let-7e in HSPCs [71, 72, 78]; miR-99b and let-7e also exhibited increased mean expression in CD34⁺CD45⁻ adherent cells, but were not statistically significant in this population. In human cord blood, miR-126 expression is highest in HSPCs with repopulating capacity in immune-deficient mouse transplants [79], while expression is significantly decreased in myeloid [79] and megakaryocyte differentiation [80]. MiR-155 negatively regulates myelopoiesis and erythropoiesis in human CD34⁺ HSPCs [81]. MiR-24 is associated with inhibition of proliferation during terminal differentiation in hematopoietic and other cell lineages [82], and is required for hematopoiesis from mouse ESCs, as suppression of miR-24 results in decreased SCL and RUNX1 expression and inhibition of HSPC production from mouse ESC-derived hemangioblasts [83]. Together, expression of these microRNAs is consistent with both the endothelial and hemogenic properties observed in the day 22 CD34⁺CD45⁻ cells. However, this hemogenic population did not express detectable miR-142-5p, in contrast to previous

reports that the development of hemangioblasts or hemogenic endothelium correlates with the emergence of low levels of miR-142-5p expression in those cells in *Xenopus*, mouse [84], and zebrafish [85]. This suggests either that hemogenic activity in the current study was only present in a small subset of the day 22 CD34⁺CD45⁻ cell population, rendering miR-142 expression undetectable in the population as a whole, or that hemogenic activity from this population only emerged during subsequent culture. Further, this data suggests a potential target through which hematopoiesis might be enhanced, by manipulating expression of miR-142 in iPSC-derived CD34⁺CD45⁻ endothelial cells.

Although the iPSC-derived CD34⁺CD45⁺ HSPCs in our study expressed HSPC-associated surface markers and transcription factors and possessed hematopoietic CFU capacity *in vitro*, these cells exhibited decreased expression of HSPC-associated microRNAs compared to CD34⁺CD45⁻ cells. The only significantly increased hematopoietic-associated microRNA expressed in day 22 CD34⁺CD45⁻ cells relative to undifferentiated iPSCs was erythrocyte-associated miR-144 [86–88], while miR-142-3p/5p and miR-223 exhibited a trend towards increased expression that fell short of statistical significance in this cell population. The decreased expression of HSPC microRNAs and increased expression of both PU.1 and microRNAs associated with maturing hematopoietic lineages (miR-142-3p/5p, miR-144, and miR-223) is consistent with the rapid differentiation of CD34⁺CD45⁺ cells and decline in CFU potential that we observed as Stage-3 culture progressed after day 22. These disparities between iPSC-derived HSPCs and their somatic counterparts may provide insights into their inability to engraft in immunodeficient NSG mice, and suggest potential molecular targets for manipulating expression to enhance their hematopoietic stem cell functions.

Conclusion

Our study provides the first detailed characterization of changes in hematopoietic cell surface phenotypes, appearance of clonogenic progenitors, and the expression of transcription factors and microRNAs during the development of HSPCs and differentiation of neutrophils from human iPSCs. While the surface marker and transcription factor expression profiles of the cell populations analyzed in this study were predominantly consistent with those expected for hemogenic endothelium, HSPCs, or maturing granulocytes, microRNA expression analyses of iPSC-derived HSPCs revealed disparities that may provide insights into the differences between these cells and their somatic cell counterparts. These findings may serve as a guide for the stem cell research community in developing tools to manipulate the production of hematopoietic cells from iPSCs.

Supplementary Material

Refer to Web version on PubMed Central for supplementary material.

Acknowledgments

This work was supported by the Intramural Research Program, National Institute of Allergy and Infectious Diseases, National Institutes of Health, projects Z01-AI-000644 and Z01-AI-000988, and by intramural awards from the National Institute of Diabetes and Digestive and Kidney Diseases to DGW and from the NIH Center for Regenerative Medicine to HLM.

References

1. Woods N-B, Parker AS, Moraghebi R, et al. Brief report: efficient generation of hematopoietic precursors and progenitors from human pluripotent stem cell lines. *Stem Cells*. 2011; 29:1158–1164. [PubMed: 21544903]
2. Hong S-H, Werbowetski-Ogilvie T, Ramos-Mejia V, et al. Multiparameter comparisons of embryoid body differentiation toward human stem cell applications. *Stem Cell Res*. 2010; 5:120–130. [PubMed: 20605758]
3. Ramos-Mejia V, Melen GJ, Sanchez L, et al. Nodal/Activin signaling predicts human pluripotent stem cell lines prone to differentiate toward the hematopoietic lineage. *Mol Ther*. 2010; 18:2173–2181. [PubMed: 20736931]
4. Gali Z, Kitchen SG, Subramanian A, et al. Generation of T lineage cells from human embryonic stem cells in a feeder free system. *Stem Cells*. 2009; 27:100–107. [PubMed: 18974209]
5. Choi K-D, Vodyanik MA, Slukvin II. Generation of mature human myelomonocytic cells through expansion and differentiation of pluripotent stem cell-derived $\text{lin}^{-}\text{CD34}^{+}\text{CD43}^{+}\text{CD45}^{+}$ progenitors. *J Clin Invest*. 2009; 119:2818–2829. [PubMed: 19726877]
6. Dias J, Gumenyuk M, Kang H, et al. Generation of red blood cells from human induced pluripotent stem cells. *Stem Cells Dev*. 2011; 20:1639–1647. [PubMed: 21434814]
7. Senju S, Haruta M, Matsumura K, et al. Generation of dendritic cells and macrophages from human induced pluripotent stem cells aiming at cell therapy. *Gene Ther*. 2011; 18:874–883. [PubMed: 21430784]
8. Takayama N, Eto K. In vitro generation of megakaryocytes and platelets from human embryonic stem cells and induced pluripotent stem cells. *Methods Mol Biol*. 2012; 788:205–217. [PubMed: 22130710]
9. Yokoyama Y, Suzuki T, Sakata-Yanagimoto M, et al. Derivation of functional mature neutrophils from human embryonic stem cells. *Blood*. 2009; 113:6584–6592. [PubMed: 19321863]
10. Sweeney CL, Merling RK, Choi U, et al. Generation of functionally mature neutrophils from induced pluripotent stem cells. *Methods Mol Biol*. 2014:189–206. [PubMed: 24504953]
11. Zou J, Sweeney CL, Chou BK, et al. Oxidase-deficient neutrophils from X-linked chronic granulomatous disease iPS cells: functional correction by zinc finger nuclease-mediated safe harbor targeting. *Blood*. 2011; 117:5561–5572. [PubMed: 21411759]
12. Medvinsky A, Dzierzak E. Definitive hematopoiesis is autonomously initiated by the AGM region. *Cell*. 1996; 86:897–906. [PubMed: 8808625]
13. Zambidis ET, Oberlin E, Tavian M, et al. Blood-forming endothelium in human ontogeny: lessons from in utero development and embryonic stem cell culture. *Trends Cardiovasc Med*. 2006; 16:95–101. [PubMed: 16546690]
14. Bertrand JY, Chi NC, Santoso B, et al. Haematopoietic stem cells derive directly from aortic endothelium during development. *Nature*. 2010; 464:108–111. [PubMed: 20154733]
15. Kissa K, Herbomel P. Blood stem cells emerge from aortic endothelium by a novel type of cell transition. *Nature*. 2010; 464:112–115. [PubMed: 20154732]
16. Zape JP, Zovein AC. Hemogenic endothelium: Origins, regulation, and implications for vascular biology. *Semin Cell Dev Biol*. 2011; 22:1036–1047. [PubMed: 22001113]
17. Kennedy MD, Souza SL, Lynch-Kattman M, et al. Development of the hemangioblast defines the onset of hematopoiesis in human ES cell differentiation cultures. *Blood*. 2006; 109:2679–2687. [PubMed: 17148580]
18. Tian X, Woll PS, Morris JK, et al. Hematopoietic engraftment of human embryonic stem cell-derived cells is regulated by recipient innate immunity. *Stem Cells*. 2006; 24:1370–1380. [PubMed: 16456127]
19. Ji J, Vijayaragavan K, Bosse M, et al. OP9 stroma augments survival of hematopoietic precursors and progenitors during hematopoietic differentiation from human embryonic stem cells. *Stem Cells*. 2008; 26:2485–2495. [PubMed: 18669904]
20. Slukvin II. Hematopoietic specification from human pluripotent stem cells: current advances and challenges toward de novo generation of hematopoietic stem cells. *Blood*. 2013; 122:4035–4046. [PubMed: 24124087]

21. Wang L, Menendez P, Shojaei F, et al. Generation of hematopoietic repopulating cells from human embryonic stem cells independent of ectopic *HOXB4* expression. *J Exp Med*. 2005; 201:1603–1614. [PubMed: 15883170]
22. Ledran MH, Krassowska A, Armstrong L, et al. Efficient hematopoietic differentiation of human embryonic stem cells on stromal cells derived from hematopoietic niches. *Cell Stem Cell*. 2008; 3:85–98. [PubMed: 18593561]
23. Amabile G, Welner RS, Nombela-Arrieta C, et al. In vivo generation of transplantable human hematopoietic cells from induced pluripotent stem cells. *Blood*. 2013; 121:1255–1264. [PubMed: 23212524]
24. Hiramoto T, Ebihara Y, Mizoguchi Y, et al. Wnt3a stimulates maturation of impaired neutrophils developed from severe congenital neutropenia patient-derived pluripotent stem cells. *Proc Natl Acad Sci USA*. 2013; 110:3023–3028. [PubMed: 23382209]
25. Gori JL, Butler JM, Chan Y-Y, et al. Vascular niche promotes hematopoietic multipotent progenitor formation from pluripotent stem cells. *J Clin Invest*. 2015; 125:1243–1254. [PubMed: 25664855]
26. Merling RK, Sweeney CL, Choi U, et al. Transgene-free iPSCs generated from small volume peripheral blood nonmobilized CD34⁺ cells. *Blood*. 2013; 121:e98–107. [PubMed: 23386128]
27. Yu J, Vodyanik MA, Smuga-Otto K, et al. Induced pluripotent stem cell lines derived from human somatic cells. *Science*. 2007; 318:1917–1920. [PubMed: 18029452]
28. Mak KS, Funnell APW, Pearson RCM, et al. PU. 1 and haematopoietic cell fate: dosage matters. *Int J Cell Biol*. 2011; 2011:808524. [PubMed: 21845190]
29. Reddy VA, Iwama A, Iotzova G, et al. Granulocyte inducer C/EBP α inactivates the myeloid master regulator PU. 1: possible role in lineage commitment decisions. *Blood*. 2002; 100:483–490. [PubMed: 12091339]
30. Karpurapu M, Wang X, Deng J, et al. Functional PU. 1 in macrophages has a pivotal role in NF- κ B activation and neutrophilic lung inflammation during endotoxemia. *Blood*. 2011; 118:5255–5266. [PubMed: 21937699]
31. Morosetti R, Park DJ, Chumakov AM, et al. A novel, myeloid transcription factor, C/EBP ϵ , is upregulated during granulocytic, but not monocytic, differentiation. *Blood*. 1997; 90:2591–2600. [PubMed: 9326225]
32. Lekstrom-Himes JA. The role of C/EBP ϵ in the terminal stages of granulocyte differentiation. *Stem Cells*. 2001; 19:125–133. [PubMed: 11239167]
33. Lengerke C, Daley GQ. Autologous blood cell therapies from pluripotent stem cells. *Blood Rev*. 2010; 24:27–37. [PubMed: 19910091]
34. Anokye-Danso F, Trivedi Chinmay M, Juhr D, et al. Highly efficient miRNA-mediated reprogramming of mouse and human somatic cells to pluripotency. *Cell Stem Cell*. 2011; 8:376–388. [PubMed: 21474102]
35. Kuo C-H, Deng JH, Deng Q, et al. A novel role of miR-302/367 in reprogramming. *Biochem Biophys Res Commun*. 2012; 417:11–16. [PubMed: 22138244]
36. Subramanyam D, Lamouille S, Judson RL, et al. Multiple targets of miR-302 and miR-372 promote reprogramming of human fibroblasts to induced pluripotent stem cells. *Nat Biotechnol*. 2011; 29:443–448. [PubMed: 21490602]
37. Larsen MT, Hother C, Häger M, et al. MicroRNA profiling in human neutrophils during bone marrow granulopoiesis and in vivo exudation. *PLoS One*. 2013; 8:e58454. [PubMed: 23554893]
38. Krishnan K, Steptoe AL, Martin HC, et al. miR-139-5p is a regulator of metastatic pathways in breast cancer. *RNA*. 2013; 19:1767–1780. [PubMed: 24158791]
39. Liu R, Yang M, Meng Y, et al. Tumor-suppressive function of miR-139-5p in esophageal squamous cell carcinoma. *PLoS One*. 2013; 8:e77068. [PubMed: 24204738]
40. Shen K, Mao R, Ma L, et al. Post-transcriptional regulation of the tumor suppressor miR-139-5p and a network of miR-139-5p-mediated mRNA interactions in colorectal cancer. *FEBS Journal*. 2014; 281:3609–3624. [PubMed: 24942287]
41. Li D, Zhao Y, Liu C, et al. Analysis of miR-195 and miR-497 expression, regulation and role in breast cancer. *Clin Cancer Res*. 2011; 17:1722–1730. [PubMed: 21350001]

42. Zhao, W-y; Wang, Y.; An, Z-j, et al. Downregulation of miR-497 promotes tumor growth and angiogenesis by targeting HDGF in non-small cell lung cancer. *Biochem Biophys Res Commun.* 2013; 435:466–471. [PubMed: 23673296]
43. Furuta M, Kozaki K-i, Tanimoto K, et al. The tumor-suppressive *miR-497-195* cluster targets multiple cell-cycle regulators in hepatocellular carcinoma. *PLoS One.* 2013; 8:e60155. [PubMed: 23544130]
44. Guo ST, Jiang CC, Wang GP, et al. MicroRNA-497 targets insulin-like growth factor 1 receptor and has a tumour suppressive role in human colorectal cancer. *Oncogene.* 2013; 32:1910–1920. [PubMed: 22710713]
45. Mestdagh P, Fredlund E, Pattyn F, et al. MYCN/c-MYC-induced microRNAs repress coding gene networks associated with poor outcome in MYCN/c-MYC-activated tumors. *Oncogene.* 2010; 29:1394–1404. [PubMed: 19946337]
46. Schulte JH, Marschall T, Martin M, et al. Deep sequencing reveals differential expression of microRNAs in favorable versus unfavorable neuroblastoma. *Nucleic Acids Res.* 2010; 38:5919–5928. [PubMed: 20466808]
47. Hamfjord J, Stangeland AM, Hughes T, et al. Differential expression of miRNAs in colorectal cancer: comparison of paired tumor tissue and adjacent normal mucosa using high-throughput sequencing. *PLoS One.* 2012; 7:e34150. [PubMed: 22529906]
48. Li FQ, Xu B, Wu YJ, et al. Differential microRNA expression in signet-ring cell carcinoma compared with tubular adenocarcinoma of human gastric cancer. *Genet Mol Res.* 2015; 14:739–747. [PubMed: 25730011]
49. Butz H, Likó I, Cziráj S, et al. MicroRNA profile indicates downregulation of the TGF β pathway in sporadic non-functioning pituitary adenomas. *Pituitary.* 2011; 14:112–124. [PubMed: 21063788]
50. Bolukbasi MF, Mizrak A, Ozdener GB, et al. miR-1289 and “zipcode”-like sequence enrich mRNAs in microvesicles. *Mol Ther Nucleic Acids.* 2012; 1:e10. [PubMed: 23344721]
51. Merkerova M, Belickova M, Bruchova H. Differential expression of microRNAs in hematopoietic cell lineages. *Eur J Haematol.* 2008; 81:304–310. [PubMed: 18573170]
52. Bissels U, Wild S, Tomiuk S, et al. Combined characterization of microRNA and mRNA profiles delineates early differentiation pathways of CD133⁺ and CD34⁺ hematopoietic stem and progenitor cells. *Stem Cells.* 2011; 29:847–857. [PubMed: 21394831]
53. Wang X-S, Gong J-N, Yu J, et al. MicroRNA-29a and microRNA-142-3p are regulators of myeloid differentiation and acute myeloid leukemia. *Blood.* 2012; 119:4992–5004. [PubMed: 22493297]
54. Jin HL, Kim JS, Kim YJ, et al. Dynamic expression of specific miRNAs during erythroid differentiation of human embryonic stem cells. *Mol Cells.* 2012; 34:177–183. [PubMed: 22767248]
55. Fazi F, Rosa A, Fatica A, et al. A minicircuitry comprised of microRNA-223 and transcription factors NFI-A and C/EBP α regulates human granulopoiesis. *Cell.* 2005; 123:819–831. [PubMed: 16325577]
56. Fukao T, Fukuda Y, Kiga K, et al. An evolutionarily conserved mechanism for microRNA-223 expression revealed by microRNA gene profiling. *Cell.* 2007; 129:617–631. [PubMed: 17482553]
57. Luis Tiago C, Naber Brigitta AE, Roozen Paul PC, et al. Canonical Wnt signaling regulates hematopoiesis in a dosage-dependent fashion. *Cell Stem Cell.* 2011; 9:345–356. [PubMed: 21982234]
58. Bigas A, Àlex R-M, Espinosa L. The Notch pathway in the developing hematopoietic system. *Int J Dev Biol.* 2010; 54:1175–1188. [PubMed: 20711994]
59. Goldman DC, Bailey AS, Pfaffle DL, et al. BMP4 regulates the hematopoietic stem cell niche. *Blood.* 2009; 114:4393–4401. [PubMed: 19759357]
60. Edvardsson L, Dykes J, Olsson ML, et al. Clonogenicity, gene expression and phenotype during neutrophil versus erythroid differentiation of cytokine-stimulated CD34⁺ human marrow cells *in vitro*. *Br J Haematol.* 2004; 127:451–463. [PubMed: 15521924]
61. Chen MJ, Yokomizo T, Zeigler BM, et al. Runx1 is required for the endothelial to haematopoietic cell transition but not thereafter. *Nature.* 2009; 457:887–891. [PubMed: 19129762]

62. Zhang Y, Payne KJ, Zhu Y, et al. *SCL* expression at critical points in human hematopoietic lineage commitment. *Stem Cells*. 2005; 23:852–860. [PubMed: 15917481]
63. Patterson LJ, Gering M, Patient R. *Scl* is required for dorsal aorta as well as blood formation in zebrafish embryos. *Blood*. 2005; 105:3502–3511. [PubMed: 15644413]
64. Shivdasani RA, Mayer EL, Orkin SH. Absence of blood formation in mice lacking the T-cell leukaemia oncoprotein tal-1/*SCL*. *Nature*. 1995; 373:432–434. [PubMed: 7830794]
65. Lacaud G, Gore L, Kennedy M, et al. *Runx1* is essential for hematopoietic commitment at the hemangioblast stage of development in vitro. *Blood*. 2002; 100:458–466. [PubMed: 12091336]
66. Lancrin C, Sroczynska P, Stephenson C, et al. The haemangioblast generates haematopoietic cells through a haemogenic endothelium stage. *Nature*. 2009; 457:892–895. [PubMed: 19182774]
67. Friedman AD. Transcriptional control of granulocyte and monocyte development. *Oncogene*. 2007; 26:6816–6828. [PubMed: 17934488]
68. Flynt AS, Lai EC. Biological principles of microRNA-mediated regulation: shared themes amid diversity. *Nat Rev Genet*. 2008; 9:831–842. [PubMed: 18852696]
69. Navarro F, Lieberman J. Small RNAs guide hematopoietic cell differentiation and function. *J Immunol*. 2010; 184:5939–5947. [PubMed: 20483778]
70. Poliseno L, Tuccoli A, Mariani L, et al. MicroRNAs modulate the angiogenic properties of HUVECs. *Blood*. 2006; 108:3068–3071. [PubMed: 16849646]
71. Guo S, Lu J, Schlanger R, et al. MicroRNA miR-125a controls hematopoietic stem cell number. *Proc Natl Acad Sci USA*. 2010; 107:14229–14234. [PubMed: 20616003]
72. Gerrits A, Walasek MA, Olthof S, et al. Genetic screen identifies microRNA cluster 99b/let-7e/125a as a regulator of primitive hematopoietic cells. *Blood*. 2011; 119:377–387. [PubMed: 22123844]
73. Harris TA, Yamakuchi M, Ferlito M, et al. MicroRNA-126 regulates endothelial expression of vascular cell adhesion molecule 1. *Proc Natl Acad Sci USA*. 2008; 105:1516–1521. [PubMed: 18227515]
74. Durrans A, Stuhlmann H. A role for *Egfl7* during endothelial organization in the embryoid body model system. *J Angiogenes Res*. 2010; 2:4. [PubMed: 20298530]
75. Huang X, Gschwend E, Van Handel B, et al. Regulated expression of microRNAs-126/126* inhibits erythropoiesis from human embryonic stem cells. *Blood*. 2010; 117:2157–2165. [PubMed: 21163928]
76. Zhu N, Zhang D, Chen S, et al. Endothelial enriched microRNAs regulate angiotensin II-induced endothelial inflammation and migration. *Atherosclerosis*. 2011; 215:286–293. [PubMed: 21310411]
77. Landgraf P, Rusu M, Sheridan R, et al. A mammalian microRNA expression atlas based on small RNA library sequencing. *Cell*. 2007; 129:1401–1414. [PubMed: 17604727]
78. Emmrich S, Rasche M, Schöning J, et al. *miR-99a/100_125b* tricistrons regulate hematopoietic stem and progenitor cell homeostasis by shifting the balance between TGF β and Wnt signaling. *Genes Dev*. 2014; 28:858–874. [PubMed: 24736844]
79. Gentner B, Visigalli I, Hiramatsu H, et al. Identification of hematopoietic stem cell-specific miRNAs enables gene therapy of globoid cell leukodystrophy. *Sci Transl Med*. 2010; 2:58ra84.
80. Garzon R, Pichiorri F, Palumbo T, et al. MicroRNA fingerprints during human megakaryocytopoiesis. *Proc Natl Acad Sci USA*. 2006; 103:5078–5083. [PubMed: 16549775]
81. Georgantas RW, Hildreth R, Morisot S, et al. CD34+ hematopoietic stem-progenitor cell microRNA expression and function: A circuit diagram of differentiation control. *Proc Natl Acad Sci USA*. 2007; 104:2750–2755. [PubMed: 17293455]
82. Lal A, Navarro F, Maher CA, et al. miR-24 inhibits cell proliferation by targeting E2F2, MYC, and other cell-cycle genes via binding to “seedless” 3'UTR microRNA recognition elements. *Mol Cell*. 2009; 35:610–625. [PubMed: 19748357]
83. Roy L, Bikorimana E, Lapid D, et al. MiR-24 is required for hematopoietic differentiation of mouse embryonic stem cells. *PLoS Genet*. 2015; 11:e1004959. [PubMed: 25634354]
84. Nimmo R, Cia-Uitz A, Ruiz-Herguido C, et al. miR-142-3p controls the specification of definitive hemangioblasts during ontogeny. *Dev Cell*. 2013; 26:237–249. [PubMed: 23911199]

85. Lu X, Li X, He Q, et al. *miR-142-3p* regulates the formation and differentiation of hematopoietic stem cells in vertebrates. *Cell Res.* 2013; 23:1356–1368. [PubMed: 24165894]
86. Papapetrou EP, Korkola JE, Sadelain M. A genetic strategy for single and combinatorial analysis of miRNA function in mammalian hematopoietic stem cells. *Stem Cells.* 2010; 28:287–296. [PubMed: 19911427]
87. Rasmussen KD, Simmini S, Abreu-Goodger C, et al. The miR-144/451 locus is required for erythroid homeostasis. *J Exp Med.* 2010; 207:1351–1358. [PubMed: 20513743]
88. Dore LC, Amigo JD, dos Santos CO, et al. A GATA-1-regulated microRNA locus essential for erythropoiesis. *Proc Natl Acad Sci USA.* 2008; 105:3333–3338. [PubMed: 18303114]

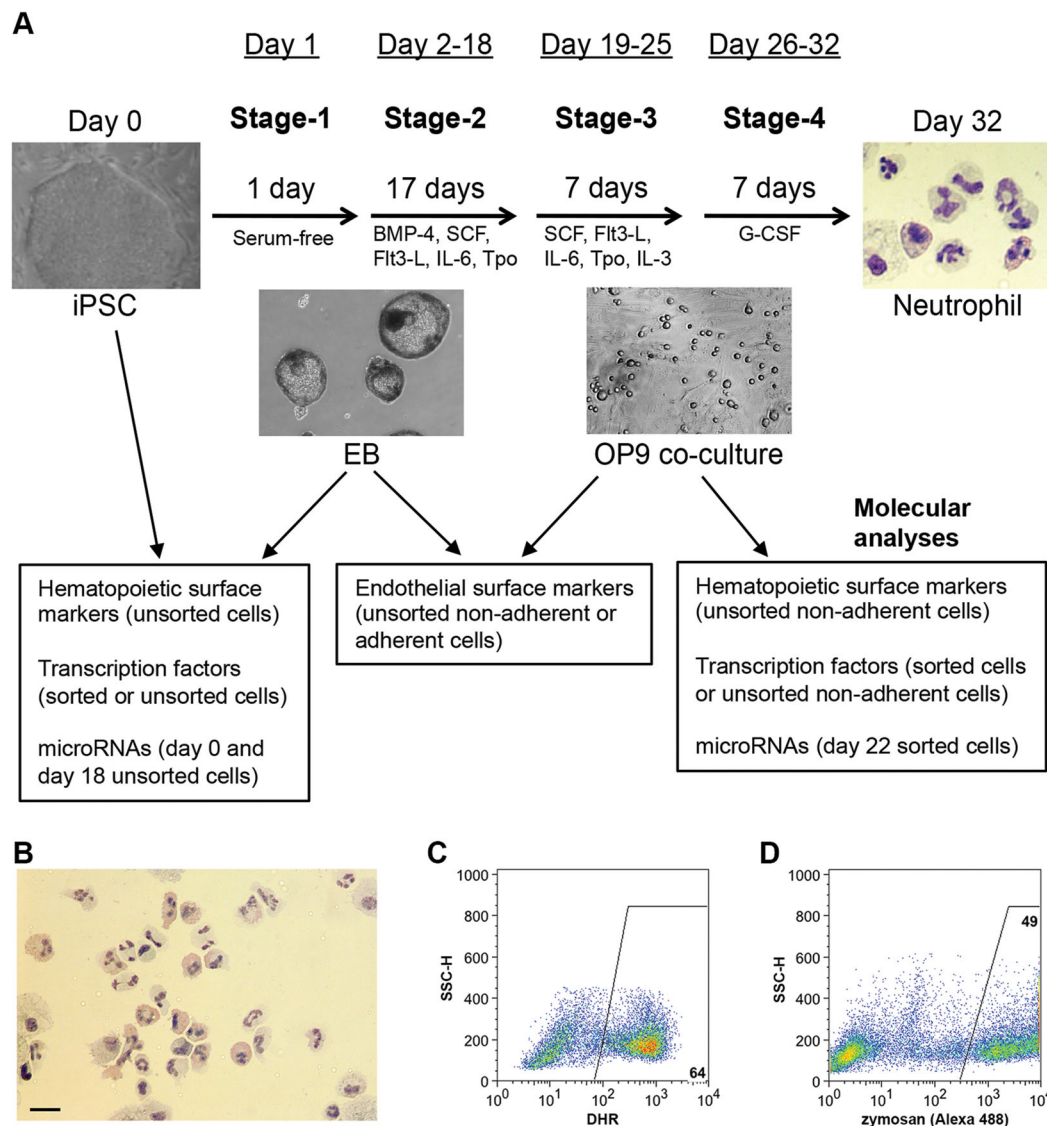


Figure 1.

In vitro directed differentiation of human iPSCs into neutrophils. (A) Schematic of the 4-stage differentiation protocol for generating mature neutrophils from iPSCs. Time-points and cytokine conditions for each stage are indicated, and representative cell images at various stages are shown. Throughout the text, day 0 refers to undifferentiated iPSCs; days 2–18 refer to cells from Stage-2 EBs; Stage-3 samples (days 19–25) refer only to the non-adherent cells from OP9 co-culture, unless specifically indicated that the adherent layer from Stage-3 was analyzed; Stage-4 samples (days 26–32) refer only to non-adherent cells. Molecular analyses of the expression of surface markers, transcription factors, and microRNAs were performed on sorted or unsorted cells from adherent, non-adherent, or total cell populations, as indicated. Images were acquired by light microscopy at 40x (iPSC and EB), 100x (OP9 co-culture) or 200x (Neutrophil; Giemsa stain) original magnification. (B) Giemsa stained cytopspin preparation of day 32 end Stage-4 differentiated cells showing cells with multilobed nucleus typical of mature neutrophil phenotype by light microscopy (bar = 20

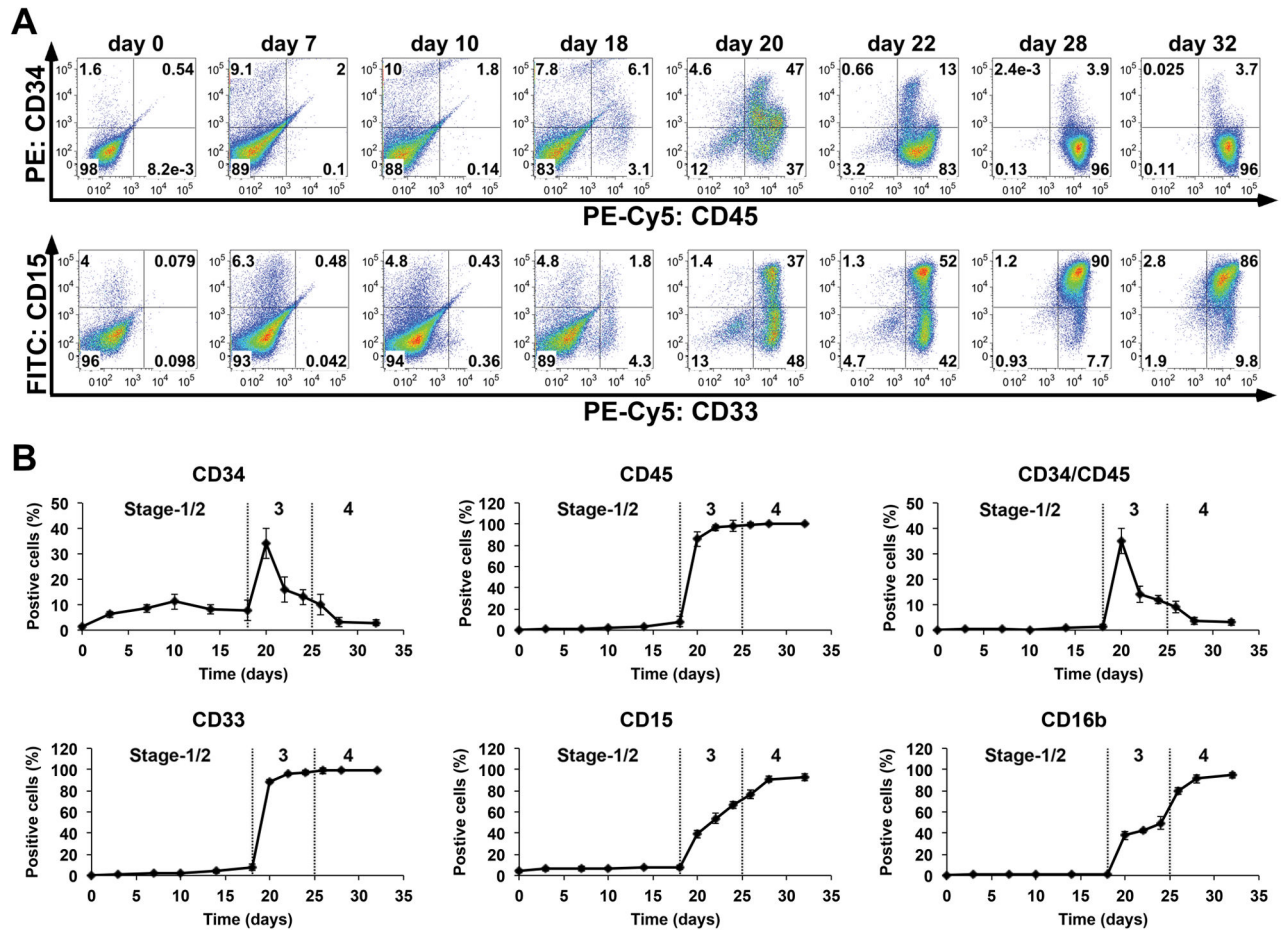
µm; 200x original magnification). Also present in this cytospin are polymorphonuclear eosinophils with red-staining granules and large mononuclear macrophages. (C) DHR flow cytometry assay of oxidase activity demonstrating that 64% of cells in the day 32 culture of neutrophils differentiated from normal iPSCs are strongly oxidase positive when maximally stimulated with phorbol myristate acetate. (D) Flow cytometry assay of phagocytosis of Alexa Fluor 488 fluorescence labeled opsonized zymosan by neutrophils present in day 32 differentiation culture.

Author Manuscript

Author Manuscript

Author Manuscript

Author Manuscript

**Figure 2.**

Hematopoietic surface marker analysis of cells during neutrophil differentiation from iPS(IMR90) and iNC-01-12 iPSCs. (A) Dot plot representation of flow cytometry analysis of cells from the indicated days (day 0, 7, 10, 18, 20, 22, 28, and 32 of differentiation) for kinetics of co-expression of HSPC surface markers CD34/CD45 or myeloid surface markers CD15/CD33. (B) Percentage of cells positive for CD34, CD45, CD34/CD45, CD33, CD15 and CD16b at days 0, 3, 7, 10, 14, 18, 20, 22, 24, 26, 28, and 32 (n=3 for each time-point; replicates were from iPS(IMR90) and iNC-01-12 iPSC lines; error bars denote standard deviation). The day 20 through day 32 data points for both panels A and B represent only analysis of the non-adherent fraction of the Stage-3 and Stage-4 cultures. Transitions between Stages-1/2, Stage-3, and Stage-4 are denoted by dotted lines.

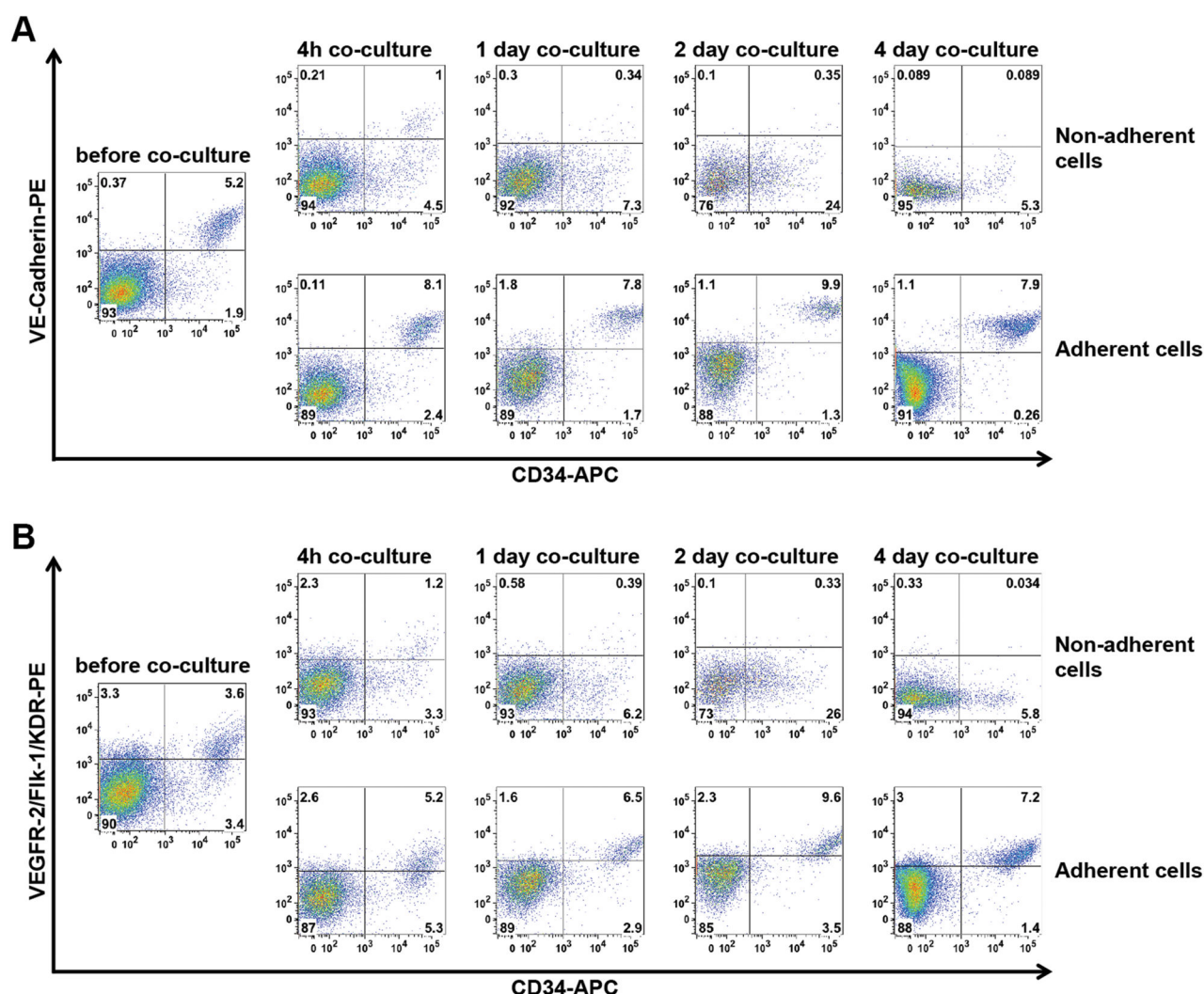
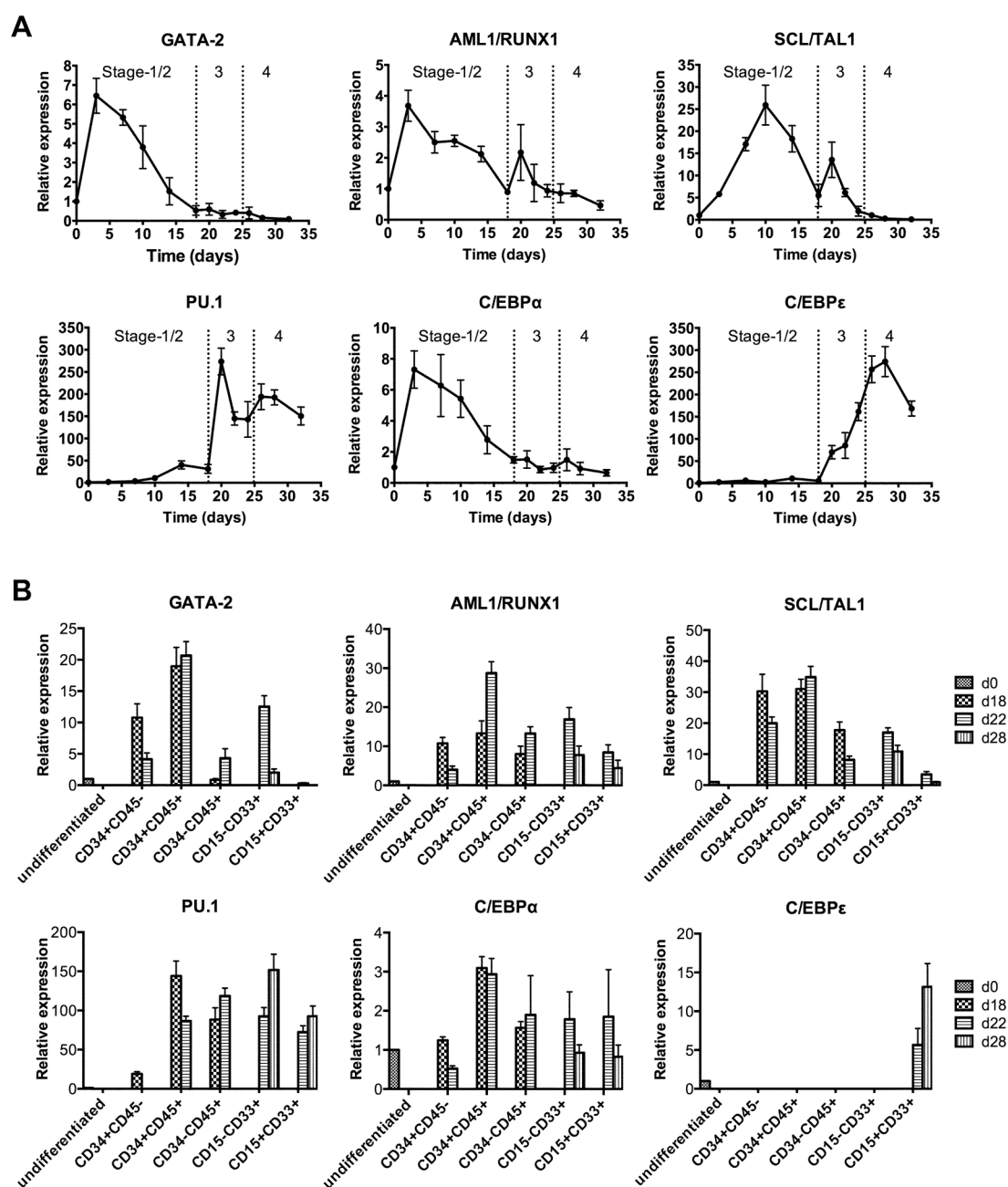


Figure 3.

Expression of endothelial surface markers before and following transition to the Stage-3 OP9 cell co-culture from iPS(IMR90) and iNC-01-12 iPSCs. At day 18, 19, 20, and 22, non-adherent cells and adherent cells were stained separately for CD34 and (A) VE-cadherin or (B) VEGFR-2/Flk-1. The left-most graph in both represents analysis of all cells in the day 18 Stage-2 culture, while the upper and lower set of graphs in both represent the non-adherent cells or tightly adherent cells respectively at 4 hours and 1–4 days after transition to the Stage-3 co-culture with OP9 cells.

**Figure 4.**

Expression kinetics of selected transcription factors during granulocyte differentiation from iPS(IMR90) and iNC-01-12 iPSCs. (A) Time course quantitative reverse-transcription PCR analysis of expression of the indicated transcription factors throughout the 4-stage differentiation culture. Expression of GATA-2, AML1/RUNX1, SCL/TAL1, PU.1, C/EBPα and C/EBPε (n=3 for each time-point; replicates from iPS(IMR90) and iNC-01-12 iPSC lines; error bars denote standard deviation) are shown relative to expression levels in undifferentiated iPSCs (day 0). Transitions between Stages-1/2, Stage-3, and Stage-4 are denoted by dotted lines. Day 3 through day 18 (Stage-2) analyses assessed all cells in the EB

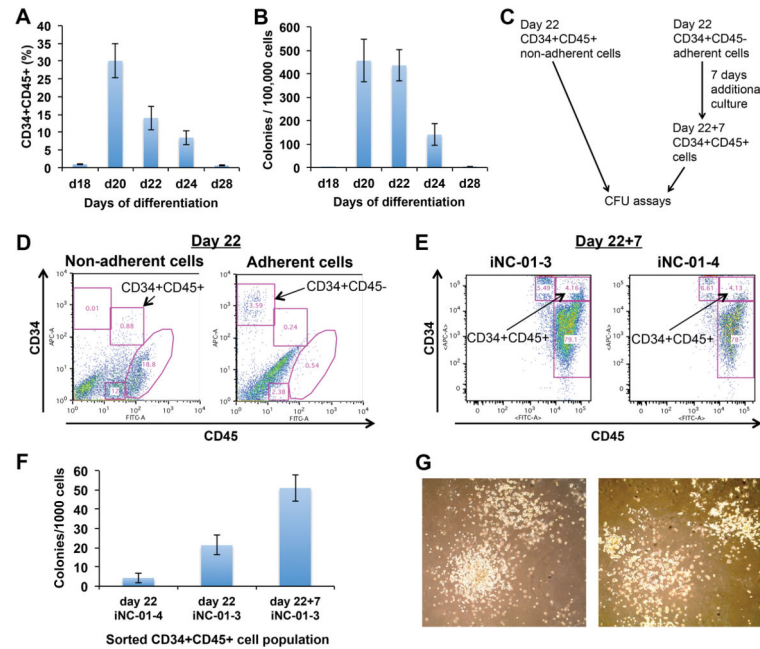
culture, but day 20 through day 32 (Stage-3 and Stage-4) analyses assessed only the non-adherent cells from OP9 culture. (B) Relationship between sorted cells expressing surface markers CD34/CD45 or CD15/CD33 and transcription factor gene expression in those cells at different days during differentiation. Quantitative reverse-transcription PCR was used to analyze the gene expression of the indicated transcription factors in the indicated sorted cell populations at day 18, 22, or 28 (d18, d22, or d28; n=3 for each population; replicates were from iPS(IMR90) and iNC-01-12 iPSC lines; error bars denote standard deviation) relative to gene expression or background levels in undifferentiated iPSCs (day 0; d0).

Author Manuscript

Author Manuscript

Author Manuscript

Author Manuscript

**Figure 5.**

Hematopoietic colony-forming potential of cells during neutrophil differentiation from iPSCs. (A) CD34/CD45 co-expression on cells used in (B) for hematopoietic CFU assays ($n=3$ for each time-point; error bars denote standard deviation), for either the total population (day 18) or non-adherent subset (days 20–28). (B) Hematopoietic colony-forming kinetics of differentiated cells on indicated days ($n=3$ for each time-point; replicates from iPS(IMR90) and iNC-01-12 iPSCs; error bars denote standard deviation). (C) Schematic of experimental design for (D–G). (D) CD34⁺CD45[−] and CD34⁺CD45⁺ cells were sorted from mid-Stage-3 (day 22 overall) differentiation cultures for CFU assays or further expansion for 7 days in Stage-3 medium without OP9 cell co-culture. Left and right panels show non-adherent and adherent cells, respectively. Data shown is from iNC-01-3 iPSCs. (E) Flow cytometry analysis of CD34 and CD45 surface marker expression after 7 days of post-sort culture of day 22 sorted CD34⁺CD45[−] cells (day 22+7). Analysis was performed in harvested pooled adherent and non-adherent cells. Left and right panels show differentiated cells from iNC-01-3 and iNC-01-4 iPSCs, respectively. (F) Hematopoietic CFU assays of CD34⁺CD45⁺ cells sorted from either day 22 or day 22+7 (day 22 CD34⁺CD45[−] cells cultured for 7 additional days in Stage-3 medium then sorted again for CD34⁺CD45⁺). iNC-01-3 and iNC-01-4 denote the iPSC line used for differentiation. (G) CFU-GM containing granulocytes and macrophages; shown are CFUs from iNC-01-3 day 22 (left panel) and day 22+7 CD34⁺CD45⁺ cells (right panel). Images were collected with an Olympus IX70 inverted microscope and FX1520 SPOT Flex Color camera (75x magnification).

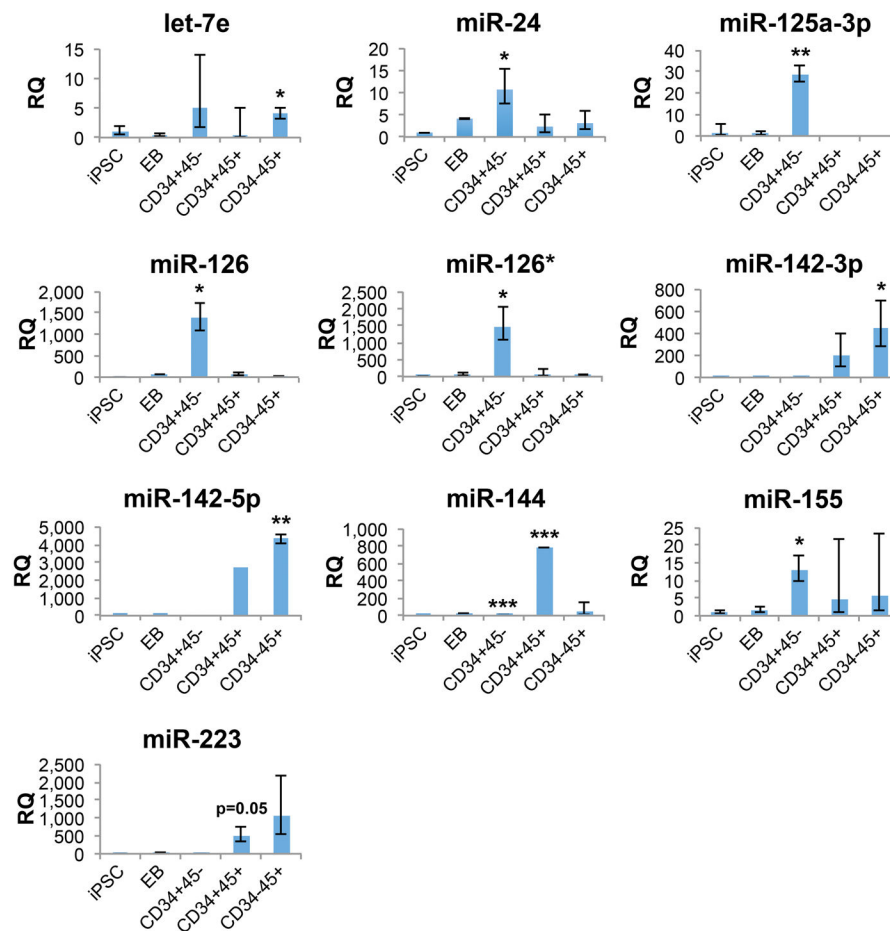


Figure 6.

Comparison of relative expression levels of selected hematopoietic-associated microRNAs between populations. Populations are undifferentiated iPSCs (iPSC), day 18 EBs (EB) and sorted day 22 cells: CD34⁺CD45⁻ adherent cells (CD34+45-), CD34⁺CD45⁺ non-adherent cells (CD34+45+), and CD34⁻CD45⁺ non-adherent cells (CD34-45+). Expression levels are relative to undifferentiated iPSCs; day 22 sorted populations with statistically significant increased microRNA expression relative to undifferentiated iPSCs are noted (*p<0.05; **p<0.01; ***p<0.001, based on ExpressionSuite two-tailed Student's t-test analysis). Samples used for microRNA analyses were biological replicates obtained from separate differentiations of iNC-01-3 and iNC-01-4 iPSCs (n=3 for day 22 samples; n=2 for EB samples; n=5 for undifferentiated iPSCs). For miR-144 in CD34+45- and CD34+45+ cells, determination of statistically significant increased expression was based on two analyzed replicates, after a third replicate with an undetermined CT was omitted by software analysis under a presumption of technical failure of the assay. Error bars denote the calculated maximum (RQ Max) and minimum (RQ Min) expression levels calculated based on 1 standard deviation; these error bars are asymmetrical due to conversion of log-based CT values to linear RQ values. Populations lacking error bars are those for which only one replicate exhibited detectable expression of the microRNA.

Author Manuscript

Author Manuscript

Author Manuscript

Author Manuscript

Table 1
MicroRNAs with significantly increased or decreased expression in day 22 populations relative to iPSCs

CD34⁺CD45⁻ adherent cells (CD34+CD45⁻), CD34⁺CD45⁺ non-adherent cells (CD34+CD45⁺), and CD34⁻CD45⁺ non-adherent cells (CD34⁻CD45⁺) were sorted from mid-Stage-3 (day 22), corresponding to the time frame of peak HSPC CFU potential in these studies. Listed are microRNAs exhibiting significantly increased or decreased expression relative to iPSCs (p<0.05, based on ExpressionSuite two-tailed Student's t-test analysis) for each day 22 sorted population. MicroRNAs that have previously been associated with hematopoiesis are listed in bold; microRNAs previously associated with pluripotency are in italics. Samples used for microRNA analyses were biological replicates obtained from separate differentiations of iNC-01-3 and iNC-01-4 iPSCs (n=3 for day 22 samples; n=2 for EB samples; n=5 for undifferentiated iPSCs). ExpressionSuite software analysis omitted any microRNA replicates in which the CT was undetermined; for some microRNAs, this resulted in a determination of statistically significant increased expression based on only two analyzed replicates (denoted by †).

Population	Significantly increased	Significantly decreased			
CD34+CD45-	miR-15a	miR-181c	miR-31	miR-205	miR-512-3p
	miR-24	miR-191* [†]	miR-93*	miR-211	miR-515-5p
	miR-28-3p	miR-195	miR-106b*	miR-222*	miR-517a
	miR-29c* [†]	miR-197	miR-127	<i>miR-302a*</i>	miR-517b
	miR-30d	miR-213	miR-129-3p	<i>miR-302b</i>	miR-518e
	miR-30e-3p	miR-326	miR-133a	<i>miR-302c</i>	miR-519a
	miR-99b*	miR-342-3p	miR-134	<i>miR-302d</i>	miR-522
	miR-122 [†]	miR-374b* [†]	miR-135a	miR-335*	miR-539
	miR-125a-3p	miR-454	miR-135b	<i>miR-367</i>	miR-543
	miR-126	miR-497	miR-135b*	<i>miR-372</i>	miR-596
	miR-126*	miR-501	miR-142-3p	miR-379	miR-622
	miR-139-5p	miR-505	miR-146a	miR-409-3p	miR-674
	miR-144[†]	miR-645	miR-149	miR-410	miR-942
	miR-145*	miR-938 [†]	miR-190	miR-411	miR-1244
	miR-151-3p	miR-941 [†]	miR-193b	miR-433	miR-1290
	miR-155	miR-1201 [†]	miR-200c	miR-487b	
	miR-181a-2*	miR-1289 [†]	miR-204	miR-495	
CD34+CD45+	miR-21 [†]	miR-146b	miR-18a	miR-93	
	miR-27a [†]	miR-191	miR-20b	miR-151-3p	
	miR-30a-5p	miR-628-3p [†]	miR-31		

Author Manuscript

Author Manuscript

Author Manuscript

Author Manuscript

Population	Significantly increased	Significantly decreased
CD34-CD45+	miR-144 [†]	
	let-7e	miR-130a
	miR-15a* [†]	miR-342-3p
	miR-16	miR-505* [†]
	miR-24-2* [†]	miR-548c
		miR-579 [†]
	miR-140-3p	miR-629-3p [†]
	miR-142-3p	miR-661 [†]
	miR-142-5p	miR-671-3p [†]
	miR-148b [†]	miR-1233 [†]
	miR-181a	miR-1260
	miR-191	miR-1291 [†]
	miR-222	miR-129-3p
		miR-17
		miR-19b
		miR-20a
		miR-20b
		miR-29a
		miR-31
		miR-31*
		miR-101
		miR-200b
		miR-204
		miR-296
		miR-301b
		miR-363*
		miR-367
		miR-543
		miR-596
		miR-744*
		miR-885-5p
		miR-935
		miR-1180